TABLE III
PASSIVE COMPENSATION

	SIMULATION WITH THE MODEL OF FIG. 2(b)		SIMULATION WITH TEN RC SECTIONS FOR EACH DISTRIBUTED RC	
	Q	f_0(KHz)	Q	f_0(KHz)
BEFORE COMPENSATION	4.621	99.70	4.631	99.80
AFTER COMPENSATION	4.022	99.75	4.029	99.85
AFTER COMPENSATION AND ADJUSTMENT OF C	4.026	100.00	4.029	100.00

loop can be found to be, after some algebra:

$$\phi = -2\left(\frac{\omega}{\omega_t}\right) - \frac{\omega}{3\omega_d} + \omega C_c R_T. \tag{10}$$

Setting this equal to zero we obtain the value of the passive compensation capacitor C_c:

$$C_c = \frac{1}{R_t}\left(\frac{2}{\omega_t} + \frac{1}{3\omega_d}\right). \tag{11}$$

For the above example, including both nonideal op amps and transistor distributed capacitances, we find $C_c = 0.129$ pF. The results of computer simulation are shown in Table III. As seen, the above approximate analysis gives a value for C_c which corrects Q almost exactly (if desired, one can improve Q further by slightly modifying C_c).

One should pay attention to the fact that the passive compensation can correct the Q of the filter, but cannot correct the center frequency value. We can use the formula for ω_0 to adjust the biquad capacitor C to move f_0 to 100 KHz. For the element values used we simply have ω_0 as given by (6), and thus we obtain the new value of C, denoted by C', by using $C'/C = 99.75/100$, giving $C' = 3.97$ pF. This method gives $f_0 = 100.00$ kHz with $Q = 4.026$ for the above example. Similar results are obtained if, instead of using a compensation capacitor, one uses "frequency predistortion" techniques by slightly modifying the values of C and R_2.

Finally, we briefly discuss the effects of the lack of perfect tracking between filter capacitors and transistor distributed capacitances. Thus, let us assume that filter capacitors are 10-percent smaller than above, while the distributed capacitances are unchanged. Then, simulation gives $f_0 = 111.10$ kHz and $Q = 4.036$. However, on an actual chip the control voltage on the gate of the transistors would automatically adjust the filter resistance to keep f_0 tuned at 100 kHz; when this is done, we obtain $f_0 = 100.00$ kHz and $Q = 3.994$. It is thus seen that, in this low-Q application, the lack of perfect tracking between filter capacitances and transistor distributed capacitances is not a problem. This effect should carefully be considered, though, for more critical applications.

V. CONCLUSIONS

The Tow–Thomas biquad, implemented in fully integrated form using MOSFET's and capacitors, has been considered at high frequencies. It was seen that, in addition to op amp finite gain-bandwidth effects, a very important effect that must be considered is due to the distributed RC nature of the MOS transistor. Taking both effects into account, formulae were derived for the deviation of the quality factor and the center frequency. These formulae take a very simple form under certain conditions. A comparison to computer simulation results showed that the formulas give satisfactory predictions, provided ω/ω_t and $Q^2\omega/6\omega_d$ are small. Simulation indicated that op amp output resistance and lumped parasitic capacitance effects for the case considered are rather unimportant, compared to the above effects. Correction of $\Delta Q/Q$ and $\Delta f_0/f_0$ can be accomplished either by using a passive compensation capacitor and adjusting one element value, or by using no such capacitor and adjusting two elements values.

REFERENCES

[1] M. Banu and Y. Tsividis, "An elliptic continuous-time CMOS filter with on-chip automatic tuning," *IEEE J. Solid-State Circuits*, vol. SC-20, Dec. 1985.

[2] Y. Tsividis, M. Banu, and J. Khoury, "Continuous-time MOSFET-C filters in VLSI," *IEEE Trans. Circuits Syst.*, vol. CAS-33, no. 6, pp. 1114–1124 Feb. 1986.

[3] J. Khoury, B. X. Shi, and Y. Tsividis, "Considerations in the design of high frequency fully integrated continuous-time filters," Proc. 1985 *ISCAS*, pp. 1439–1442, Kyoto, Japan.

[4] J. Tow, "Active *RC* filters—A state space realization," *Proc. IEEE*, vol. 56, pp. 1137–1139, 1968.

[5] L. C. Thomas, "The biquad; Part I and Part II," *IEEE Trans. Circuit Theory*, vol. CT-18, pp. 350–361, May 1971.

[6] M. S. Ghausi and J. J. Kelly, *Introduction to Distributed-Parameter Networks: With Application to Integrated Circuits*. New York: Holt, Reinehart, and Winston, 1968.

[7] A. S. Sedra and P. O. Brackett, *Filter Theory and Design: Active and Passive*. Beaverton, OR: Matrix, 1978.

Components Quantization Effects on Continuous-Time Filters

JAIME RAMÍREZ-ANGULO, RANDALL L. GEIGER, AND EDGAR SÁNCHEZ-SINENCIO

***Abstract*—Recent trends in precision continuous-time active filter design use post fabrication tunable structures. Digitally adjustable quantization components are often used as tunable elements. It is shown that the trim resolution of continuous-time filters is strongly dependent upon the circuit topology and component quantization schemes. Tradeoffs between number of bits, quantization schemes and resolution for some representative bandpass active filter structures are addressed. It is shown that the optimal circuit structure and component quantization scheme are application dependent.**

I. INTRODUCTION

Programmable filters [1]–[3] find use in a wide variety of applications spanning the areas of audio, instrumentation, communications, medical electronics, etc. Digital control of the filter characteristics is a desirable feature that can be used for very accurate parameter setting. Digital control also allows for digital system compatibility of the analog filter structures. The quantization of the component values of an active filter results in filters

Manuscript received July 31, 1985.

The authors are with the Department of Electrical Engineering, Texas A&M University, College Station, TX 77843-3128.

IEEE Log Number 8608538.

which are characterized by a discrete set of attainable values for the filter characteristics of interest such as the pole frequency ω_0, the pole quality factor Q, etc.

One popular way to digitally control the characteristics of an active filter is through the use of multiplying digital to analog converters (MDAC's) driving an operational amplifier (op amp) structure [4]. This combination can be used to implement digitally adjustable gain blocks, integrators, lossy integrators and summers. In these blocks the MDAC works essentially as a binarily weighted resistance. In [5] and [6], second-order structures using MDAC's for independent control of ω_0 and Q are compared. The structures are based on the state-variable realization in [5], and on structures which use two finite gain blocks in [6] which are noted for inherently high sensitivities. Emphasis is placed on limitations imposed by the nonideal performance characteristics of the MDAC-op amp combination. The tuning scheme adopted in these comparison requires a minimum of two op amps for all structures.

A more general scheme for achieving digitally tunable active filters involves quantizing components by replacing some or all of the elements in any existing active filter structure with digitally controlled and weighted capacitor or resistor arrays. From a practical viewpoint, those active filters which offer independent ω_0 and Q adjustment may prove easier to tune. The previously discussed implementation with MDAC's can be considered to be a particular implementation leading to a component quantization scheme with the resistors taking uniformly distributed values according to the binary law:

$$R = R_0\left(2^{-1}d_1 + 2^{-2}d_2 + \cdots + 2^{-N}d_N\right).$$

where R_0 determines the adjustment range and $d_1, d_2, \cdots, d_N$ represents the binary input. In any case, the set of all possible quantization combinations for the components of any filter structure is mapped into a discrete set of pole locations in the s-plane.

A popular approach for implementing tunable filters is based on the state-variable realization [2]–[4], [7]. This is due primarily to attractive tunability characteristics, favorable sensitivities, and the flexibility for obtaining simultaneously BP, LP, and HP transfer characteristics.

When designing digitally tunable active filters the following questions naturally arise:

1) What circuit topology is best suited for digital control?
2) Where are the poles and zeros of a specific structure located for a given number of bits and a given quantization scheme?
3) Which components should be digitally controlled?
4) What is the optimal component quantization scheme for a given filter structure?

Coefficient quantization effects in digital filters have been investigated by several researchers [8]. Little has been reported on component quantization effects on continuous time filters. Previous papers have mainly concentrated on the use and limitations of the MDAC. It will be shown in this paper that the tuning range and parameter resolution of digitally tuned continuous-time filter structures depends primarily and interactively upon the filter structure and the component quantization schemes. Component range, functional component value-filter characteristic relationship, number of components, interdependence of parameters, and component sensitivity must be considered when selecting a filter structure suitable for digital control. The choice of the structure will be strongly dependent upon the required filter specifications. Filters with large component variations or many components should be avoided in monolithic applications due to large area requirements associated with practical realizations. Parameter independence will allow for convenient adjustment of the filter characteristics by individual components, possibly at the expense of increased cost or decreased performance capabilities. Parameter independence does not guarantee attractive component value-filter characteristic relationships. Functional component value-filter characteristic relationships will affect the resolution of the filter structure.

Circuits with low component sensitivities may prove useful for practically making small local adjustments but are inherently unsuitable for global adjustments of filter characteristics. Conversely, circuits with high component sensitivity allow for global parameter adjustment with modest changes in component values but have poor resolution.

In this paper, we address the previously posed questions by showing a comparative study of the root loci for several representative second-order active filter structures obtained using a combination of two basic component quantization schemes. The aim of this study is to show, in addition to the other well known properties of the different biquadratic structures discussed, that the root loci as determined by component quantization must be considered as a important factor when selecting a filter structure for a specific digitally tunable application. It will be shown that root loci give information not necessarily obtainable from classical sensitivity measures. Differences in the root loci associated with narrow and wide tuning range applications, effects of quantization schemes and the need to include the distribution of ω_0 and Q must be considered when optimizing digitally controlled filter designs.

II. Basic Quantization Schemes

Two basic quantization schemes for obtaining a component value X within a prespecified range $[X_{\min}, X_{\max}]$ are considered here:

a) A direct quantization scheme where the 2^N discrete values of X are distributed uniformly in the closed interval $[X_{\min}, X_{\max}]$ according to the expression:

$$X = X_{\min} + \Delta X\left[2^0 d_1 + 2^1 d_2 + \cdots + 2^{N-1} d_N\right] \tag{1}$$

where $X_{\min}$ and $X_{\max}$ are the minimum and maximum values needed for the variation of the component, N is the number of bits in the digital word $\boldsymbol{d} = d_1, d_2, \cdots, d_N$, and the incremental value ΔX is given by

$$\Delta X = \frac{X_{\max} - X_{\min}}{2^N - 1}. \tag{2}$$

This quantization scheme can be modeled by a series combination of resistors or by a parallel combination of capacitors, as shown in Fig. 1(a).

b) An inverse quantization scheme where the 2^N discrete values of $1/X$ are distributed uniformly over the closed interval $[1/X_{\max}, 1/X_{\min}]$ according to the expression:

$$\frac{1}{X} = \frac{1}{X_{\max}} + \frac{1}{\Delta X}\left[2^0 d_1 + 2^1 d_2 + 2^{N-1} d_N\right] \tag{3}$$

where the inverse incremental value is given in this case by

$$\frac{1}{\Delta X} = \left(\frac{1}{X_{\min}} - \frac{1}{X_{\max}}\right)\frac{1}{2^N - 1}. \tag{4}$$

This quantization scheme can be modeled by a parallel combination of resistors or by a series combination of capacitors, as shown in Fig. 1(b).

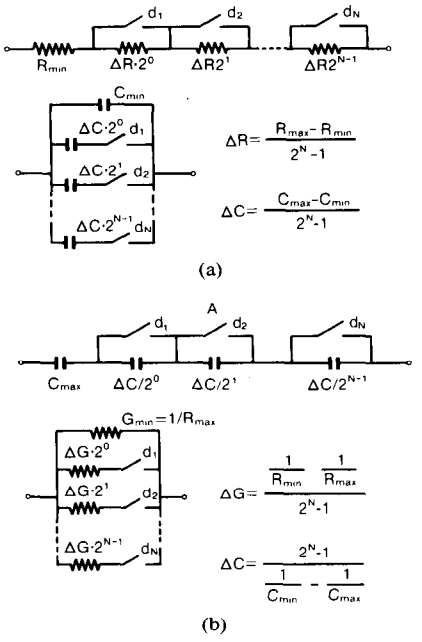

Fig. 1. Quantization scheme implementation. (a) Direct quantization scheme. (b) Inverse quantization scheme.

These schemes and interconnections of these configurations along with $R-2R$ and ladder-type circuits form a small but useful subset of the infinite number of possible component quantization structures. The networks shown in Fig. 1(a) and 1(b) are not intended to be practical implementations of these quantization schemes but are rather used to model the specific quantization strategy. The synthesis of practical quantization structures is beyond the scope of this paper.

III. Comparative Study of RC-Active Filter Structures

The effects of any component quantization scheme on any filter structure are difficult to address in the general sense. The importance of the component quantization strategy on circuit can however be readily demonstrated by example. Examples emphasizing the interrelationships between circuit topology and component quantization scheme are presented in this section.

A comparative study of the performance of four popular biquadratic filter structures [9] is now made by using combinations of the two basic switching arrangements of Fig. 1 from both a local (narrow tuning range) and a global (wide tuning range) viewpoint. The biquad structures considered for this study are the bandpass version of the Sallen and Key, the Friend–Deliyannis,[1] the GIC implementation and the KHN-State-Variable filters. The specific structures along with design equations for independent control of ω_0 and Q are shown in Fig. 2. These were chosen for illustrative purposes so that single, double, and multiple amplifier structures were represented in the comparative study. They also represent structures with practical relationships between component values and the filter characteristics which are typically of interest. In all structures a resistor ratio, K, a set of resistors or a set of capacitor values which allow for independent

[1]Although it has been shown that the Friend–Deliyannis and the Sallen and Key structures are complementary [10], [11] and therefore their poles are given by the same relationships, the complementary transformation does not preserve the zeros of the transfer function that are obtained when elements are lifted off ground, the complement of the bandpass circuit of Fig. 2(a) is the standard Sallen and Key high-pass circuit. The structures shown in Fig. 2(a) and (b) are both bandpass structures and they are not related by the complementary transformation, therefore they have different poles.

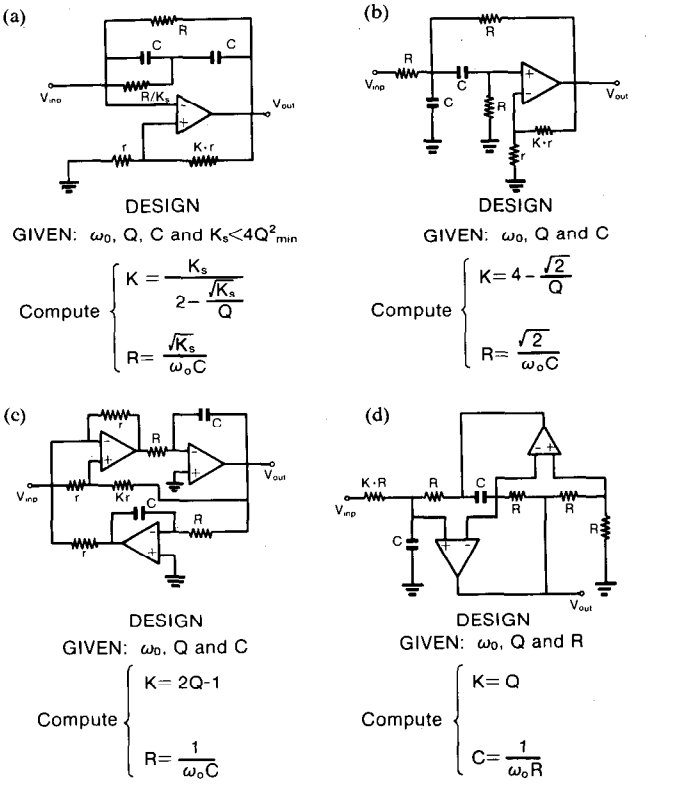

Fig. 2. Biquad bandpass RC-active structures. (a) Friend–Deliyannis. (b) Sallen and Key. (c) State variable KHN. (d) Gyrator.

ω_0 and Q adjustment were selected for digital control. For the circuits of Fig. 2(b), 2(c), and 2(d), a single resistor or capacitor value serves as a free design parameter. In addition to a passive component value, the designer has control of the positive feedback parameter, K_s, in the circuit of Fig. 2(a), which allows the designer to make tradeoffs between sensitivity and component spread [12].

ω_0 and Q Tuning Ranges

The investigation of component quantization was undertaken by assigning parameter values to K and R or C leading to root loci spanning the same region in the s-plane for all circuits in the comparison. In the global comparison, relatively wide Q and ω_0 tuning ranges were chosen with values for Q adjustable from 0.505 to 100 and ω_0 normalized adjustable over one decade from 0.1 to 1.0 rad/s. Parameter values were quantized to three bits for all structures giving a total of 64 sets of discrete pole positions. In the local comparison, ω_0 and Q were adjustable over a relative narrow range from 0.5 to 1.0 rad/s (1 octave) and from 1.5 to 6, respectively. In the Friend–Deliyannis structure, the parameter K_s was assigned a value of 1 for the global comparison and 8 for the local comparison. These values are, in both cases, close to the maximum allowed value of $4Q^2_{\min}$, where $Q_{\min}$ represents the minimum value of Q attainable with the digital control scheme.

Narrow Tuning Range Comparison

A local comparison of the pole loci of all four circuits using the direct quantization scheme for both the Q and ω_0 tuning elements is shown in Fig. 3. Fig. 4 shows a local comparison of the pole loci obtained by using the inverse quantization scheme. Note that in the first case the performance (resolution) of all structures is quite different. That is the density of the poles is very much

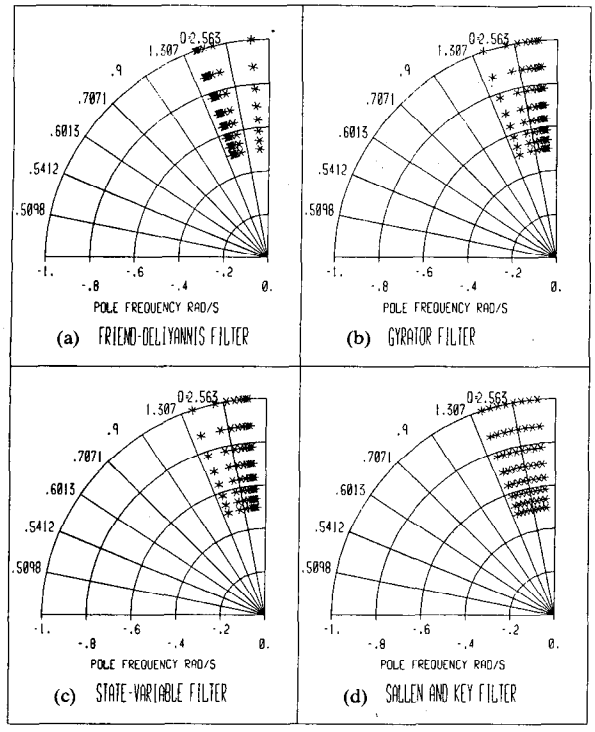

Fig. 3. Local comparison of filter structures with direct quantized component values. (a) K and R direct quantized. (b) K and C direct quantized. (c) K and R direct quantized. (d) K and R direct quantized.

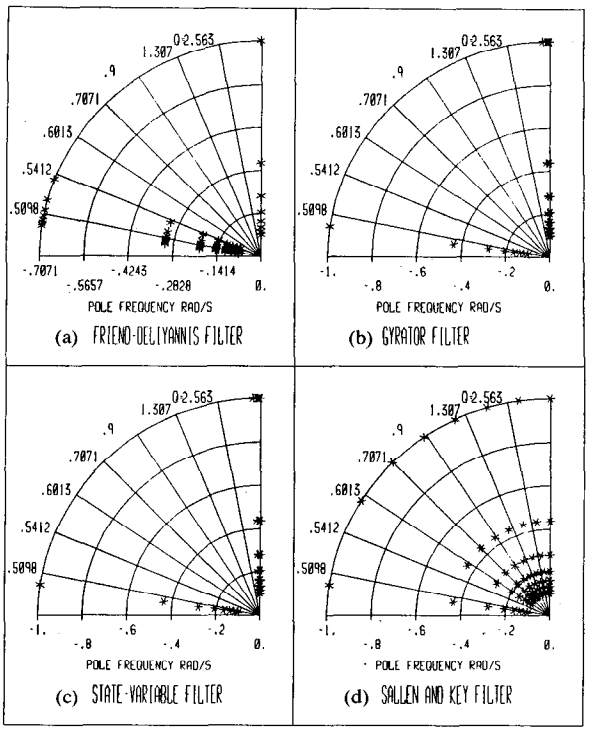

Fig. 5. Global comparison of filter structures with direct quantized components. (a) K and R direct quantized. (b) K and C direct quantized. (c) K and R direct quantized. (d) K and R direct quantized.

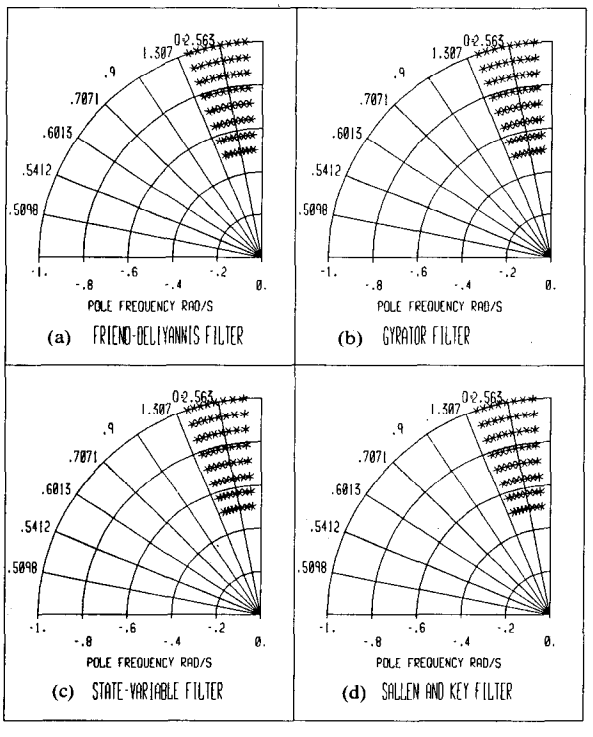

Fig. 4. Local comparison of filter structures with inverse quantized component values. (a) K and R inverse quantized. (b) K and C inverse quantized. (c) K and R inverse quantized. (d) K and R inverse quantized.

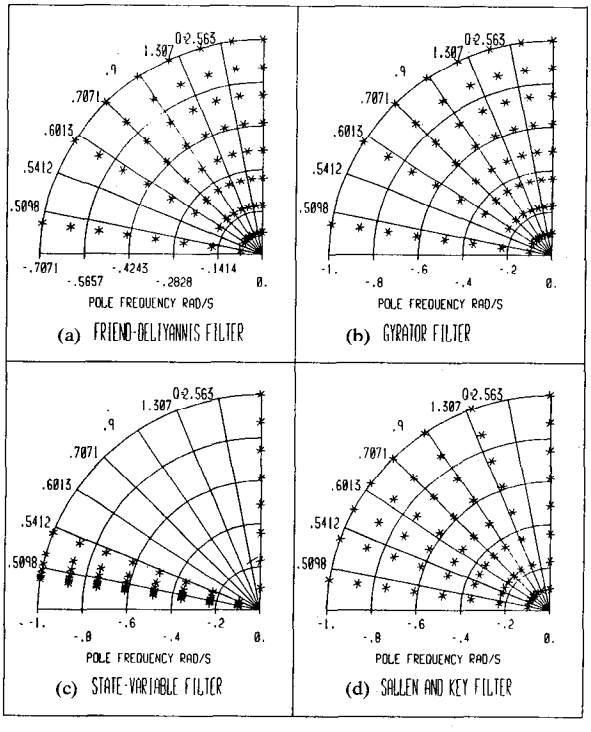

Fig. 6. Global comparison of filter structures with inverse quantized component values. (a) K and R inverse quantized. (b) K and C inverse quantized. (c) K and R inverse quantized. (d) K and R inverse quantized.

topology dependent. In the second case all structures show similar pole loci. Furthermore, by comparing results shown in Figs. 3 and 4 for the same topology it can be readily seen that resolution is a function of the quantization scheme adopted.

Wide Tuning Range Comparison

Fig. 5 shows a global comparison of the pole loci obtained by using the direct quantization scheme for K and R. It can be noted that in this case each structure shows the same basic pole

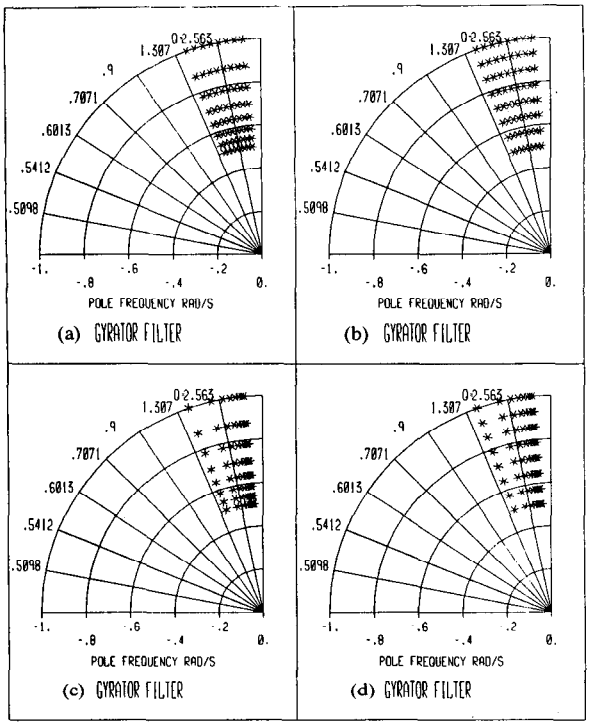

Fig. 7. Local comparison of quantization schemes for Gyrator filter. (a) K inverse C direct quantized. (b) K and C inverse quantized. (c) K and C direct quantized. (d) K direct C inverse quantized.

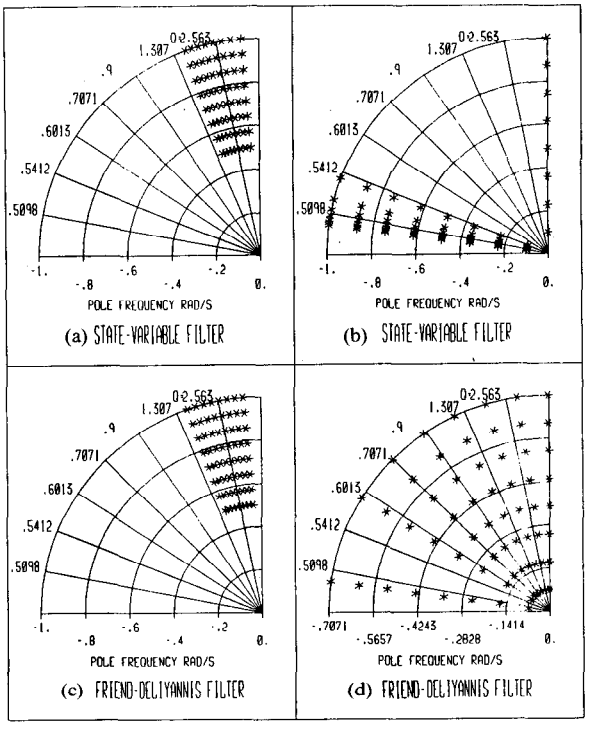

Fig. 8. Comparison of local and global performance for State-Variable and Friend–Deliyannis structures with inverse quantized component values. (a) K and R inverse quantized. (b) K and R inverse quantized. (c) K and R inverse quantized. (d) K and R inverse quantized.

distribution pattern of the local counterpart in Fig. 3 but the nonuniformities become much more accentuated. Fig. 6 shows a global comparison of the pole loci obtained by using the inverse quantization scheme for both tuning parameters K and R or C. Note here that in spite of the fact that all the structures show a similar resolution from the local point of view, in the global comparison they show quite different performance.

Component Quantization Scheme Effects

The strong influence of the quantization schemes of Fig. 1(a) and 1(b) on the pole distribution will now be considered. To illustrate these effects, the Gyrator structure is selected. In Fig. 7 local comparison of the root loci is obtained by using combinations of the two quantization schemes. The plot of Fig. 7(a) shows the effect of the direct quantization scheme for capacitor C and an inverse quantization scheme for the parameter K. In Fig. 7(b) the effect of the inverse quantization scheme for C and K is shown. Fig. 7(c) correspond to the effect of a direct quantization scheme for C and K. Finally the effect of using the inverse quantization for C and the direct quantization scheme for K is shown in Fig. 7(d). Note that even for a specific structure the resolution of the poles is strongly dependent upon the quantization scheme. Thus an alternative to choose a different circuit structure is to use a combination of different component quantization schemes. The optimal choice of quantization schemes for a given circuit is dependent upon the desired performance characteristics.

Narrow and Wide Tuning Range Comparison

Next a comparison of the local and global quantization effects is made. The State-Variable and the Friend–Deliyannis structures are compared in Fig. 8. The inverse quantization scheme of Fig. 1(b) was used to adjust all parameter values. Note that although the State-Variable structure gives reasonable resolution with this quantization scheme for local adjustment, the resolution is extremely poor for high Q values in the global case. In fact the grid is densest in the region of low Q-values. The Friend–Deliyannis structure shows a pole grid evenly distributed (relative to the linear axis) both in the global and in the local cases. This distribution might be suitable for some applications.

Considering the high-Q approximation

$$Q = \frac{1}{2\sin\alpha} \approx \frac{1}{2\alpha}$$

where α is the pole angle measured with respect to the imaginary ω-axis, it can be recognized that an inverse distribution of the values of Q corresponds to a uniform distribution of α. Thus, the analytical expressions relating Q and K given in Fig. 2 and the tuning range for K can be used to demonstrate the fact that all structures show an approximately uniform pole locus when K is adjusted with the inverse quantization scheme.

An interesting characteristic of the Sallen and Key structure, is that it shows approximately uniform pole loci both in the local and global sense and for K adjusted with either the direct or inverse quantization scheme. Fig. 9(a) and 9(b) shows local and global root loci for a direct quantization of K. Fig. 9(c) and 9(d), show local and global root loci for an inverse quantization of K. In all cases R is quantized with the inverse quantization scheme.

Although we have restricted this comparison to 3-bit quantization schemes and to a global tuning range of one decade, it has been observed that increasing the number of bits leads to a denser pole grid following the same pole distribution pattern and that widening the tuning range leads to root loci showing similar but more pronounced effects on the pole distribution than were observed in this comparison. It should be apparent that for a given resolution the number of bits required is strongly a func-

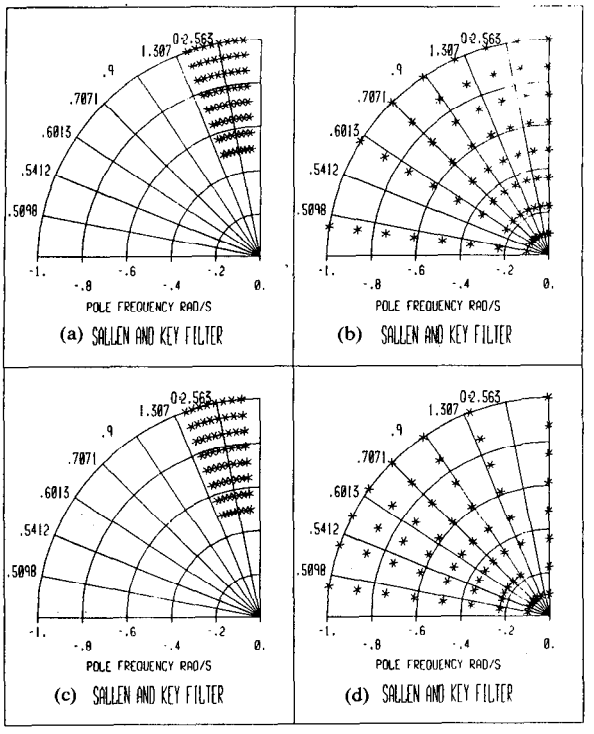

Fig. 9. Local and global comparison of quantization schemes for Sallen and Key filter. (a) K direct R inverse quantized. (b) K direct R inverse quantized. (c) K and R inverse quantized. (d) K and R inverse quantized.

tion of both the circuit structure and the quantization scheme. For instance, it can be seen from Fig. 6 that for a wide Q-tuning range application and by using the inverse quantization scheme, the State-Variable structure requires a larger number of bits than any of the other 3 structures if the same resolution in the mid- and high Q-regions is to be achieved. The selection of the optimal structure, switching arrangements and number of quantization bits must be made based primarily on the tuning range and on the specific distribution of the values of Q and ω_0 required for a particular application. The Q-distribution offered by general use commercially available tunable filter units based on the State-Variable[2] realization may be far from optimal for some specific applications. If, for example, a uniform pole distribution (in the angular sense in the s-plane) over a wide tuning range is required and K is direct quantized, it is evident from Fig. 6 that the state-variable is the least suitable structure. These aspects are discussed in more detail in Section IV.

Pole Distribution Density Functions

So far we have imposed constraints on the component values of the structures so that ω_0 and Q can be independently realized. In some applications the requirement of a pole pattern following a distribution density function in a region not necessarily limited by constant ω_0 and Q-lines can arise. In these cases, the constraint of independent control of Q and ω_0 can be disregarded. This is equivalent to having a requirement for specific pairs of $\{\omega_0, Q\}$ values rather than a particular ω_0 and a family of Q's or vice versa a particular Q and a family of ω_0's. Additional degrees of freedom can be obtained from each structure by quantizing

[2]National Semiconductor Model AF100, EG&G Reticon, R5610 Quad Programmable Fitler Array.

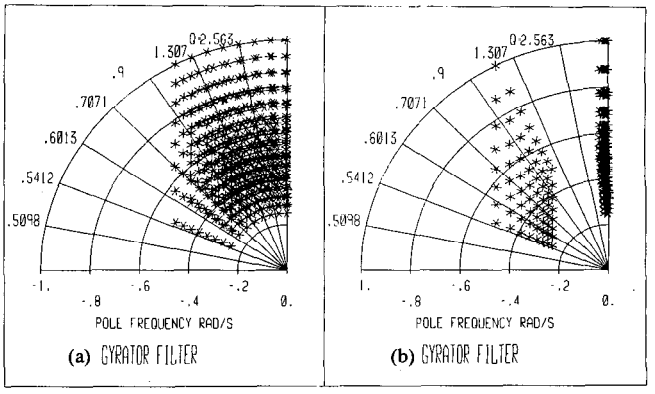

Fig. 10. Comparison of quantization schemes for the Gyrator filter with K, R, and C quantized. (a) K, C, and R inverse quantized. (b) K, C, and R direct quantized.

independently the values of all resistors and capacitors. This leads to a much larger grid of pole locations for each structure. To illustrate this, the root locus for the Gyrator filter when all parameters R, C, and K are independently quantized with the inverse quantization scheme is shown in Fig. 10(a). This quantization with 3 parameters generates 512 discrete complex-conjugate pole pairs. Fig. 10(b) shows the root locus for R, C, and K direct quantized. The component values have been chosen to have the following range: R from 1 to 2, K from 1.1 to 100, and C from 1 to 2. The component values were quantized as before with 3 bits. It can be seen that in this case the root locus is not uniformly distributed in either the radial sense (constant Q) or in the angular sense (constant ω_0).

Even more flexibility in this structure can be obtained if all component values are independently adjusted. Since this structure has 5 resistors and 2 capacitors, independent control of all components quantized to only 3 bits yields $(2^3)^7 = 2097152$ possible conjugate pole–pair combinations. The impact on the resolution and tuning range with this simple structure should be apparent. The additional degrees of freedom can allow the designer to "tailor" the root locus to best fit the pole density function required for a given application.

It is important to point out that the information obtained from the root loci plots shown here can not be derived from classical sensitivity measures. The sensitivity measures are useful for predicting approximate changes only for small parameter variations. They can therefore be used only to make predictions in the local sense. It was shown that global parameter variations can lead to radically different pole distributions than is obtained for local variations which indicates that large change sensitivities are not necessarily correlated with classical small change sensitivities.

IV. Overall Comparison between Structures for Specific Design Requirements

The circuit characteristics or specifications of interest to the designer are strongly application dependent. Some of the characteristics that are often of interest include: cutoff frequencies (linear adjustment), cutoff frequencies (logarithmic adjustment), bandwidth, ripple, pole positions, magnitude response (linear or logarithmic axis), phase response, ω_0, Q, etc. For illustrative purposes, applications requiring linear control of the quality factor Q, the normalized bandwidth BW/ω_0 and the angle α as

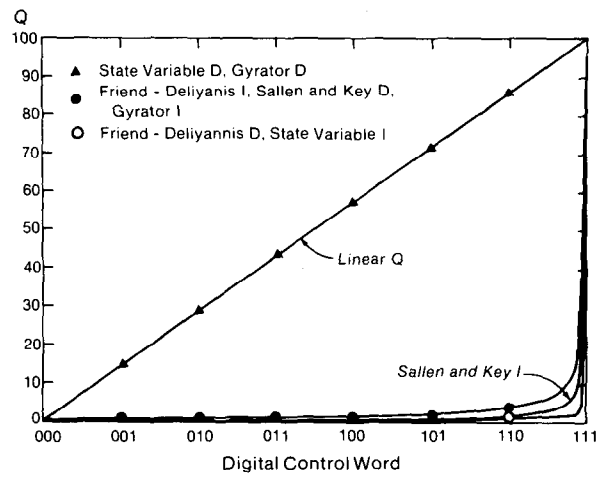

Fig. 11. Global comparison of combinations for linear Q-requirements.

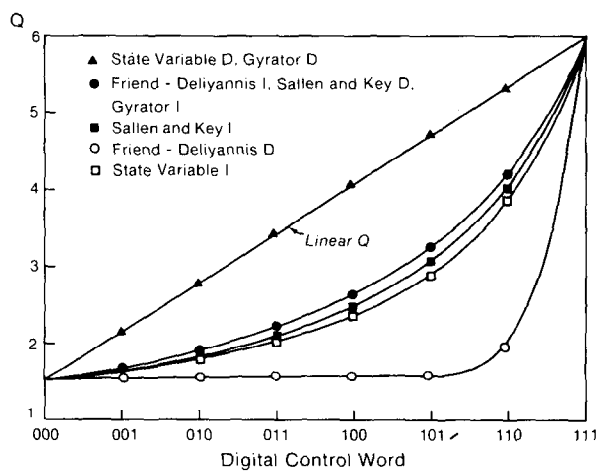

Fig. 12. Local comparison of combinations for linear Q-requirements.

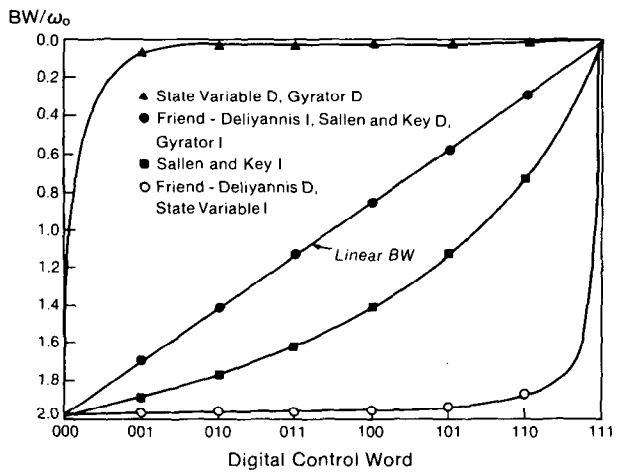

Fig. 13. Global comparison of combinations for linear BW/ω_0 requirements.

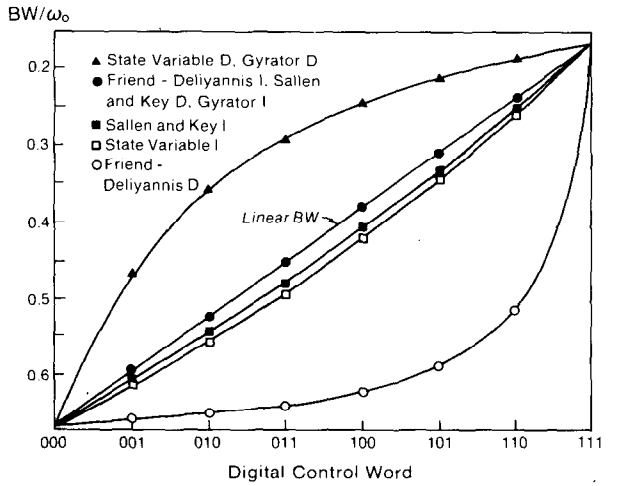

Fig. 14. Local comparison of combinations for linear BW/ω_0 requirements.

requirements for three different applications of digitally programmable filters are considered in this section. In each case it is desired to determine the structure and the quantization schemes yielding the highest resolution.

The parameters Q, BW/ω_0 and α are related to the angular distribution of poles according to the expressions:

$$Q = \frac{1}{2\sin\alpha} \tag{5}$$

$$BW/\omega_0 = 2\sin\alpha. \tag{6}$$

Again, assuming the resistors and capacitors for the circuits of Fig. 2 are constrained as indicated in the figure, it follows that only the quantization scheme for K needs to be considered since the Q parameter appears only in the expression for K. In what follows a 'combination' is denoted as a structure with a particular quantization scheme for K; for instance, the combination Gyrator D refers to the Gyrator Structure with a direct quantization scheme for K, the combination State Variable I refers to the state variable structure with an inverse quantization scheme for K.

Case 1. Linear Q: The distribution of Q-values for the 8 possible combinations of structure and quantization scheme for K are shown in Figs. 11 and 12 for the global and for the local cases respectively. Indicated on each curve are the Q-values corresponding to each of the 2^N discrete values of the digital control word for the case $N = 3$. The values of Q for different numbers of quantization bits N can be obtained from the curves shown by reading the ordinate corresponding to the subdivision of the horizontal axis in $2^N - 1$ equal intervals. For the combinations: Gyrator I, Sallen and Key I, Friend Deliyannis D and State Variable I, the digital control word is the 1's complement of the digital control word labeling the horizontal axis[3]. For a given N the Q-resolution for any combination structure-quantization scheme is obtained as the maximum vertical separation between succesive points on the corresponding curve.

Following observations can be made with respect to Figs. 11–12:

i) There are group of combinations that show essentially the same resolution both at the local and at the global level. The combinations State Variable D and Gyrator D form one such group that will be denoted as Group I, the combinations Friend–Deliyannis I, Sallen and Key D and Gyrator I form another group denoted as Group II.

[3]Ones complement was used when plotting these curves to easy interpretation of the results of the comparison.

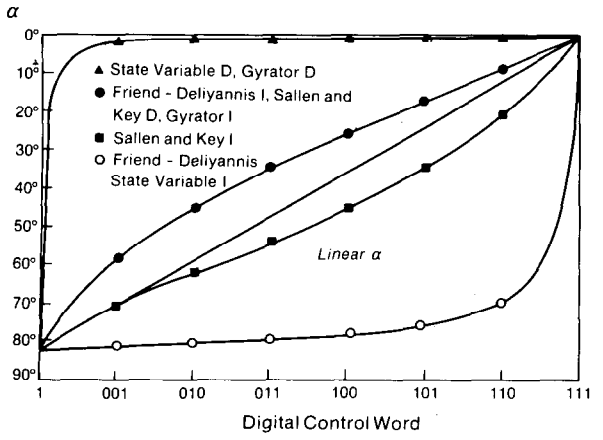

Fig. 15. Global comparison of combinations for linear α-requirements.

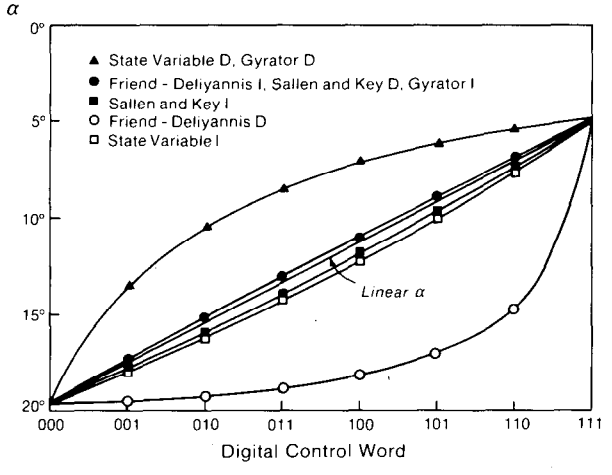

Fig. 16. Local comparison of combinations for linear α-requirements.

ii) The combinations of Group I show a linear Q distribution for both the local and global cases. The linearity of the combination Gyrator D is due to the relationship $Q = K$ for the Gyrator. The expression $Q = (K+1)/2$ for the State Variable filter may on the other hand make the results to appear surprising since apparently for low Q values a deviation from linearity should be expected. The explanation for the very good linearity of the state variable D combination even for low Q-values resides in the fact that the K_{min} and K_{max} are assigned so that the extreme values of the Q-tuning range: Q_{min} and Q_{max} are exactly obtained and so the curve for the State Variable D combination is "forced" to coincide with the linear Q-distribution. An important conclusion follows that contrary to what can be expected from the functional relationship between K and Q, both combinations in group I are very well suited for implementing circuits with linear control over Q for both local and global applications.

Case 2. Linear BW/ω_0: Figs. 13 and 14 show curves corresponding to the distribution of the BW/ω_0-values from the global and from the local point of view respectively. The same comments about the labeling of the horizontal axis as were made for Case 1 apply for these and subsequent figures. In this case it can be observed that the combinations of Group II show a linear BW/ω_0 dependence with respect to the digital control word both from the local and from the global point of view. In a local sense the combinations Sallen and Key I and State Variable I also show a reasonable resolution.

Case 3. Linear α: A comparison of the distribution of α-values obtained in the global and local case, respectively, are shown in Figs. 15 and 16 with a linear α axis. It can be seen that there is not a combination nor a group of combinations showing an exact linear α distribution. The linear α line lies between the curve of Group II and that of the Sallen and Key I combination. Since the combination Sallen and Key D belongs to Group I this suggests that a linear control over α can be best obtained with the Sallen and Key structure by adjusting K with a quantization arrangement that combines both the direct and inverse quantization schemes. At the local level the combinations of Group II provide a very good resolution. This can be explained from (5) and (6) by considering that for small values of α ($\alpha < 0.2$ rad) the bandwidth BW is approximately linearly related with α according to

$$BW \approx 2\omega_0\alpha. \tag{7}$$

Therefore, the requirements of linear control over α and BW/ω_0 coincide at the local level.

It should be apparent from these comparisons that in addition to the circuit topology and component quantization scheme, the resolution is strongly a function of the specific circuit characteristics of interest. A strategy for evaluating/comparing the performance of a given circuit structure–quantization scheme follows from the illustrative examples considered in this section. Specifically the circuit characteristic of interest[4] can be plotted against the component value which is to be adjusted. The required number of bits for a given circuit structure, quantization scheme and resolution requirement can be determined by observing the maximum functional spacing between quantized outputs as the number of bits for quantization is increased.

V. Conclusions

It has been shown by example that trim resolution of quantized trim circuit structures is strongly dependent upon both the component quantization scheme and the filter topology. Component quantization schemes on local applications may differ considerably from that observed in global applications even though the circuit topology may remain fixed. Even for a given circuit and a given component quantization scheme, the effective resolution is strongly a function of the specific circuit characteristics of interest to the user.

Although the examples were restricted to biquadratic active RC structures similar results can be obtained for higher order structures as well as for passive RLC circuits. Similar results will also be observed for digitally controlled monolithic structures even though the circuit structures and/or component quantization schemes may be quite different from those considered in the examples.

No general conclusion can be drawn regarding either the best circuit structure and the best component quantization scheme for digitally controlled applications. The importance of judiciously selecting both the circuit topology and component quantization schemes for digitally controlled filters has been demonstrated.

[4]Restricted to the range of interest and using the axis (linear, logarithmic, etc.) of interest.

REFERENCES

[1] L. T. Bruton, "Electronically tunable analog active filters," *IEEE Trans. Circuits Theory*, vol. CT-19, pp. 299–301, May 1972.
[2] R. G. Sparkes and A. S. Sedra, "Programmable active filters," *IEEE J. Solid-State Circuits*, vol. SC-8, pp. 93–95, Feb. 1973.
[3] T. A. Hamilton, "Stable, digitally programmable active circuits," *IEEE J. Solid-State Circuits*, vol. SC-9, pp. 27–28, Feb. 1974.
[4] J. J. Hill, "Digital control of active filter characteristics," *Int. J. Electron.*, vol. 41, pp. 405–410, 1976.
[5] J. Zurada, "Programmable state-variable active biquads," *J. Audio Eng. Soc.*, vol. 29, pp. 786–793, Nov. 1981.
[6] J. Zurada and K. Goodman, "Gain-tuned programmable 2nd-order filters with VCVS," *Proc. Inst. Elect. Eng.*, vol. 129, Pt. G, pp. 221–228, Oct. 1982.
[7] D. J. Allstot, R. W. Brodersen and P. R. Gray, "An electrically programmable switched capacitor filter," *IEEE J. Solid-State Circuits*, vol. SC-14, Dec. 1979.
[8] A. V. Oppenheim and R. W. Schafer, *Digital Signal Processing*. Englewood Cliffs, NJ: Prentice Hall, 1975.
[9] A. S. Sedra and P. O. Brackett, *Filter Theory and Design: Active and Passive*. Portland, OR: Matrix, 1978.
[10] A. S. Sedra, M. A. Ghorab, K. Martin, "Optimum configurations for single-amplifier biquadratic filters," *IEEE Trans. Circuits Syst.*, vol. CAS-27, 12, pp. 1155–1163, Dec. 1980.
[11] G. S. Moschytz and P. Horn, "Optimizing two commonly used active filter building blocks using a complementary transformation," in *Proc. IEEE ISCAS 1977*, pp. 332–335, Apr. 25–27, 1977.
[12] P. E. Fleischer, "Sensitivity minimization in a single amplifier biquad circuit," *IEEE Circuits Syst.*, vol. CAS-23, pp. 45–55, Jan. 1976.

Efficient Computation of Network Sensitivities

FATEHY M. EL-TURKY

***Abstract*—A class of methods for generating network functions and their sensitivities, when only one element is allowed to vary, is presented. This class of methods requires either two or three circuit analyses to obtain expressions for the network function and its first order, higher order, and large-scale sensitivities for all values of the variable component. The class of the two circuit analyses methods reduces moderately the computational effort and makes better use of circuit analysis data as compared to the previous methods which employ at least three circuit analysis. The results are applicable to network functions with bilinear characteristics and can be extended to the general class of bilinear systems.**

I. INTRODUCTION

In the past two decades the topic of network sensitivities has been investigated extensively. Efficient methods and algorithms have been developed to compute network sensitivities. The considerable progress made in the theoretical study of sensitivities, along with increased efficiency in sensitivity computation has helped give a clear insight into network function behavior when the network parameters are subject to change. Most network performance measures, whether deterministic or probabilistic, require the computation of sensitivities. In optimal tolerance assignments, and in most cases of circuit optimization, first and second order sensitivities have to be computed.

Manuscript received May 13, 1985; revised December 5, 1985.
The authors is with AT&T Bell Laboratories, Naperville, IL 60566.
IEEE Log Number 8608535.

Most of the existing methods for computing sensitivities use the concept of the "adjoint network" or equivalently the "transpose system" [1], [2], [5]. This method requires only one circuit analysis to compute all network sensitivies. Several backward and forward substitutions are needed as well. In this class of methods the solution of the original system as well as the solution of the transpose system are needed to compute sensitivities. If one element is subject to changes, the system matrix can be updated using the Householder's formula [3], and only a backward and forward substitution is needed to update all sensitivities. If all the network elements are subject to change, it may be more economical to repeat the solution than update it. In this study an attempt has been made to derive closed form expressions for sensitivities of network functions, when only one element is subject to change [4], [6], [8], [10], [15]. It is shown that only two values of the network function and the corresponding denominator or the first order sensitivity are needed to compute and update the network function and its sensitivities. The network function denominator and its first order sensitivity come as by-products during circuit analysis, and making use of them will save an extra circuit analysis. If the denominator and the first order sensitivity are not available, only three function values are needed to determine the value of the network function at any other point, and the corresponding value of all derivatives [4].

The results reported here can be easily implemented in any analysis program, particularly for symbolic function generation. This is essential in solving fault problems, where closed form expressions for various network functions are needed for efficient generation of fault dictionaries (single and double faults).

II. GENERATION OF BILINEAR NETWORK FUNCTIONS

For most of the existing linear network elements, the transfer function $F(s)$ is bilinear, with the exception of perhaps the ideal transformer turns ratio and mutual inductance. If one of the network parameters is allowed to vary while all others are kept constant, then we can write the following

$$F(s,e)=\frac{A(s)+eB(s)}{a(s)+eb(s)}=\frac{N(e,s)}{D(e,s)} \tag{1}$$

where e is the network parameter subject to change, and $A(s)$, $B(s)$, $a(s)$, and $b(s)$ are the network coefficients, which are function of the complex frequency s and the value of the other network parameters. N and D are the numerator and the denominator of F, respectively.

From (1), the sensitivity of F with respect to e can be expressed as

$$F'(e)=\frac{\partial F}{\partial e}=\frac{BD-Nb}{D^2}=\frac{aB-Ab}{D^2}=\frac{k}{D^2}. \tag{2}$$

In general analysis programs the network equations are written using the tableau or the modified tableau method. They have the form [7]

$$\boldsymbol{SX}=\boldsymbol{W} \tag{3}$$

where $\boldsymbol{S}$ is the system matrix and contains the network parame-

0098-4094/86/0700-0659$01.00